International Journal of General Medicine

Dovepress
Taylor & Francis Group

Open Access Full Text Article

ORIGINAL RESEARCH

Comprehensive Pan-Cancer Analysis Identifies IGFL1 as an Oncogenic Biomarker and Immunotherapeutic Target with Experimental Validation in Bladder Cancer

Zongjian Liang[1,*], Yu An[2,*], Jie He[2], Zhiqiang Zhu[1], Kehua Jiang[3], Kun Chen[4], Fa Sun[1]

[1]Department of Urology, The Affiliated Hospital of Guizhou Medical University, Guiyang, Guizhou, People's Republic of China; [2]NHC Key Laboratory of Pulmonary Immune-Related Diseases, Guizhou Provincial People's Hospital, Guiyang, Guizhou, People's Republic of China; [3]Department of Urology, Guizhou Provincial People's Hospital, Guiyang, Guizhou, People's Republic of China; [4]Department of Medical Genetics, Guizhou Provincial People's Hospital, Guiyang, Guizhou, People's Republic of China

*These authors contributed equally to this work

Correspondence: Kun Chen, Department of Medical Genetics, Guizhou Provincial People's Hospital, 83 Zhongshan East Road, Guiyang, Guizhou, 550081, People's Republic of China, Email 44844956@qq.com; Fa Sun, Department of Urology, the Affiliated Hospital of Guizhou Medical University, 28 Guiyi Street, Guiyang, Guizhou, 550081, People's Republic of China, Email sfgmc@sina.com

Background: IGFL1, a member of the insulin growth factor-like family, plays a potential role in tumorigenesis. This study aimed to investigate IGFL1 expression and its prognostic and immunological significance across cancers, with experimental validation in bladder cancer (BLCA).

Methods: Data from TCGA, GTEx, and TIMER2.0 were analyzed to assess IGFL1 expression across cancers and its associations with prognosis, immune subtypes, immune infiltration, and tumor-related genomic features. Drug sensitivity data were also evaluated. Given BLCA's high mutation burden, limited treatment options, and strong IGFL1 dysregulation observed in pan-cancer analysis, we selected it for experimental validation. In vitro and in vivo experiments were conducted to validate the oncogenic role of IGFL1 in BLCA and explore its underlying mechanisms.

Results: IGFL1 was significantly overexpressed in 10 tumor types and associated with advanced stage and grade in BLCA. High IGFL1 expression correlated with poor prognosis in OV, SARC, HNSC, PAAD, UCEC, KIRC, and BLCA. IGFL1 expression was linked to features of the tumor microenvironment in several cancers. In BLCA tissues, IGFL1 levels were markedly elevated. Knockdown of IGFL1 in 5637 and ScaBER cells reduced proliferation, migration, and epithelial–mesenchymal transition (EMT)-related protein expression; overexpression had the opposite effect. In vivo, IGFL1 silencing suppressed xenograft tumor growth, decreased Ki67 expression, increased apoptosis, and enhanced $CD4^+$ and $CD8^+$ T-cell infiltration. Mechanistic analysis suggested that IGFL1's effects are mediated through the JAK2/STAT3 signaling pathway.

Conclusion: IGFL1 promotes tumor progression and immune modulation in multiple cancers, particularly in BLCA. Its oncogenic and immunosuppressive roles, mediated through the JAK2/STAT3 axis, support its potential as a prognostic biomarker and therapeutic target.

Keywords: IGFL1, pan-cancer, bladder cancer, tumor immunology, tumorigenesis

Introduction

Cancer remains the primary cause of death globally, imposing a huge health and economic burden on nations each year.[1] Tumorigenesis is a multifaceted biological process that engages numerous signaling pathways and key genes, among which the tumor microenvironment (TME) plays a pivotal role.[2,3] With the advancement of resource sharing and public databases, comprehensive pan-cancer analyses of genes have become possible, providing valuable insights for identifying new targets for immunotherapy.

Received: 7 February 2025
Accepted: 10 July 2025
Published: 15 July 2025

In 2006, Peter Emtage et al discovered a human-secreted protein named the Insulin Growth Factor-Like Family. This protein family was exclusively found in humans and mice, with humans having IGFL1-4 and two pseudogenes, while mice have only mIGFL.[4] IGFL exhibits low expression in normal human tissue, with IGFL1 being detected in the ovaries and spinal cord, IGFL2 in the cerebellum, heart, placenta, spleen, stomach, testes, and thymus, and IGFL3 and IGFL4 in the cerebellum. Mohit Rajput et al found that arsenic trioxide (As2O3) induces malignant transformation in immortalized keratinocytes (HaCaT) through upregulation of IGFL1, leading to various cutaneous malignant diseases, including Bowen's disease, Merkel cell carcinoma, squamous cell carcinoma and basal cell carcinoma.[5] IGFL1 may facilitate the invasion and metastasis of lung adenocarcinoma cells by modulating EMT and mediating the AKT/mTOR signaling pathway, thus expediting the progression of lung adenocarcinoma.[6] Basal-like breast cancer denotes an exceptionally aggressive subtype of breast cancer, Wang Haixia and colleagues reported that KLF5 can induce the transcription of IGFL2-AS1 and IGFL1 in basal-like breast cancer cell lines. Additionally, under TNF-α stimulation, KLF5 and IGFL2-AS1 jointly promote IGFL1 expression. The KLF5/IGFL2-AS1/IGFL1 regulatory axis facilitates the proliferation of basal-like breast cancer cells and tumor growth.[7]

However, all existing studies on IGFL1 have been restricted to particular cancer, and no comprehensive pan-cancer studies have been conducted to investigate its expression, prognosis, and tumor immune functions. Therefore, we utilized multiple databases to analyze IGFL1 expression and its prognostic across 33 cancer types. We also examined its relationship with immune cell infiltration, immune regulatory genes, immune checkpoint genes, TMB, MSI, and other indicators. This study establishes a basis for further investigation of the oncogenic mechanisms of IGFL1.

Materials and Methods

Data Acquisition

The Xena database (https://xenabrowser.net/datapages/) integrates RNA sequencing data and clinical follow-up information from 33 types of cancer patients from TCGA. We utilized the TIMER database to analyze the differential expression of IGFL1 between tumor and normal tissues and assess its correlation with tumor-infiltrating immune cells (http://cistrome.dfci.harvard.edu/TIMER/). Given the limited number of normal tissue samples in the TCGA database, we supplemented this with normal tissue data obtained from the GTEx database. The TCGA and GTEx expression datasets were merged based on common Ensemble gene identifiers, with samples annotated by source (TCGA tumor, TCGA normal, GTEx normal) and tissue type. To ensure comparability and mitigate potential batch effects between the TCGA and GTEx cohorts, the merged expression values were log2-transformed [log2(FPKM + 1)] and subjected to ComBat batch correction using the sva R package (version 3.50.0), with data source (TCGA/GTEx) as the batch variable. The combined and normalized dataset was then statistically analyzed and visualized using R software (version 4.3.2). The mapping of tumor abbreviations to their full names in the TCGA database was shown in the Supplementary Table1.

Prognostic Value of IGFL1 in Pan-Cancer

We accessed the GEPIA2 database (GEPIA 2, cancer-pku. cn) to generate plots and perform statistical analysis on the relationship between IGFL1 expression levels and overall survival (OS) as well as relapse-free survival (RFS) in pan-cancer patients. Additionally, we employed the Kaplan-Meier Plotter (http://kmplot.com/analysis/) to calculate the optimal cutoff values and plot survival curves, thereby assessing the prognostic value of IGFL1 in selected cancer types.

Relationships Between IGFL1 Expression and Tumor Immune

TISIDB (http://cis.hku.hk/TISIDB/) was employed to analyze the tumor immune subtypes. We applied the R package "Immuneeconv", which uses TIMER and xCELL algorithms to analyze immune cell infiltration in pan-cancer samples. The "ESTIMATE" algorithm was applied to assess immune scores. We examined the association between IGFL1 expression and the expression of eight marker genes in immune checkpoint pathways, as well as immune modulator genes. Heatmaps were generated using Sangerbox (http://sangerbox.com/).

Correlation Research on IGFL1 and Tumor Heterogeneity

Tumor Mutation Burden (TMB) indicates the quantity of somatic mutations detected per million base pairs in the tumor genome, and it is often directly linked to the effectiveness of immune checkpoint inhibitor treatment.[8] Microsatellite Instability (MSI) typically arises from defects in DNA repair mechanisms or inaccurate DNA replication.[9] Homologous Recombination Deficiency (HRD) refers to defects or abnormalities in DNA damage-repairing mechanisms, contributing to tumorigenesis and progression.[10] Loss of Heterozygosity (LOH) occurs when one allele in a chromosomal region is lost while the other allele undergoes mutation or deletion. LOH is an important genetic marker closely associated with tumorigenesis and progression.[11] Mutant-Allele Tumor Heterogeneity(MATH) indicates genetic diversity among different cell populations within a tumor; high MATH values suggest greater genetic heterogeneity, which may correlate with increased tumor aggressiveness and faster progression.[12] Neoantigens are protein fragments generated by gene mutations in tumor cells absent in normal cells, making them recognizable by the immune system and potential targets for attack.[13] Tumor Purity denotes the fraction of cancerous cells present in a sample compared to normal cells or other non-tumor cells.[14] Spearman correlation analysis was utilized to explore the association between IGFL1 expression and these indices.

Drug Sensitivity Analysis

The GSCALite platform was used to assess the correlation between IGFL1 expression and responsiveness to commonly administered anticancer drugs.

Cell Culture and Transfection

All cell lines used in this study were obtained from Wuhan Pricella Biotechnology Co., Ltd (Wuhan, China) and have passed mycoplasma testing and STR identification prior to shipment. Human bladder cancer cell lines 5637 (cat:CL002) and ScaBER (cat:CL0203) were cultured in RPMI-1640 medium, while the immortalized normal urothelial cell line SVHUC (cat:CL0222) was used as a control and cultured in Ham's F-12K medium. Mouse bladder cancer cells MB49 (TCMC794) were cultured in a DMEM medium. All culture media were enriched with 10% fetal bovine serum (FBS), and cells were maintained in a humidified incubator at 37°C with 5% CO2. Small interfering RNA targeting IGFL1 (Si-IGFL1) and an overexpression plasmid (OE-IGFL1) were designed and synthesized by Sangon Biotech and transfected into cells using the Lipofectamine 2000 Kit (Thermo Fisher Scientific) in accordance with the manufacturer's instructions. After 48 hours of transfection, we detected the transfection efficiency, and subsequent functional assays were performed The sequences of the three small interfering RNAs (siRNAs) are as follows:

siRNA-1$^{\#}$: 5'-CAUGACUCCUUACCUGAUGCUTT-3'

siRNA-2$^{\#}$: 5'-GAAACUGCACCUUCAGAGUCUTT-3'

siRNA-3$^{\#}$: 5'-GAUAAACCAGAACUGCGACUTT-3'

The IGFL1-interfering lentivirus (Si-IGFL1) and IGFL1-overexpression lentivirus (OE-IGFL1) were constructed by Shanghai GenePharma Co., Ltd. and used to infect BLCA cells. The RNA sequence of the IGFL1-interfering lentivirus is identical to that of siRNA-1$^{\#}$.

RNA Sequencing

Small interfering RNA (siRNA-1$^{\#}$) was transfected into 5637 cells to knock down IGFL1 expression, with negative control as the control group. Each group had three replicates. Total RNA was extracted and sent to Guangdong Magigene Biotechnology Co., Ltd for transcriptome sequencing. Differentially expressed genes(DEGs) were pinpointed according to the significance criteria of adj-P < 0.05 and log2FC > 1. Enrichment analysis of these differential genes was performed using KEGG (https://www.kegg.jp), GO (https://geneontology.org), and GSEA (https://www.gsea-msigdb.org/gsea/index.jsp).

Functional Assays of IGFL1 in vitro

The proliferation of BLCA cells was measured with the Cell Counting Kit-8 (CCK8) assay. 5637 and ScaBER cells were incubated at 37°C. At the same time each day, CCK8 reagent was added to each well, and absorbance was recorded at

450 nm to evaluate cell growth. For the scratch wound healing assay, cells were plated for adherence. After transfection with Si-IGFL1 or OE-IGFL1, a cross-shaped scratch was generated with a 200 μL pipette tip. The cells were then cultured in a serum-free medium for another 24 hours, and images were captured to assess the extent of wound closure. Cell migration was evaluated using the Transwell assay. The upper chamber of the Transwell insert was filled with 200 μL of serum-free medium containing the cells, while the lower chamber was supplemented with 600 μL of complete medium. After migration to the lower surface, cells were fixed, stained with crystal violet, and counted across five randomly selected fields.

In vivo Experiments

The experimental animals were purchased from GemPharmatech Co., Ltd (Chengdu, China). The experiment involved 5-week-old male BALB/C-nude mice, randomly assigned to either the control or experimental group, with four in each group. Each group received a subcutaneous injection of 5637 cells infected with either control lentivirus (Si-Ctrl) or IGFL1-interfering lentivirus (Si-IGFL1), with 3.75 × 10^6 cells injected per mouse. At the same time, we also subcutaneously injected four male C57 mice (8 weeks old) with MB49 cells infected with the IGFL1-overexpression lentivirus and four other mice with control group cells. The subcutaneous tumor growth was monitored weekly, and tumor volume was calculated. After 4 weeks (2 weeks), the mice were sacrificed, and the tumors were collected. The Animal Experimental Ethical Inspection Form of Guizhou Medical University approved this study (Approval Number: 2305143).

Quantitative Real-Time Polymerase Chain Reaction (qRTPCR), Western Blot (WB) Assay, and Immunohistochemistry (IHC)

Total RNA was extracted from cells using the PureLink RNA extraction kit (Thermo Fisher Scientific). The RNA was then reverse-transcribed into cDNA using the 1st Strand cDNA Synthesis SuperMix Kit (YEASON, Shanghai, China). Quantitative PCR was performed using SYBR Green Master Mix (YEASON, Shanghai, China). The primer sequences were shown as follows:

- IGFL1 Forward: 5'-ATCTCCAGGCTCCTCTGCTCAC-3'
- IGFL1 Reverse: 5'-GGGCACGACGGCATCATCATAG-3'
- GAPDH Forward: 5'- ACACCCACTCCTCCACCTTTG −3'
- GAPDH Reverse: 5'- TCCACCACCCTGTTGCTGTAG −3'

Total protein was isolated from tissues and cells using RIPA lysis buffer. Proteins were separated by SDS-PAGE and transferred onto a PVDF membrane. Primary antibodies were applied to the membrane and left to react overnight at 4°C, including:

- IGFL1 (HUABIO, ER61595, 12 kDa,1:1000)
- E-cadherin (CST, 3195S, 110 kDa,1:5000)
- N-cadherin (HUABIO, ER0503, 110 kDa,1:2500)
- VIMENTIN (Diagbio, db30006, 54 kDa,1:1000)
- SLUG (Zenbio,350136,20kDa,1:500)
- STAT3 (Zenbio, R22785, 88 kDa,1:1000)
- phospho-STAT3 (Zenbio, 310019, 88 kDa,1:1000)
-JAK2 (HUABIO, M1501-8, 130kDa,1:1000)
-phopho-JAK2 (HUABIO, ET1607-34, 130kDa.1:1000)
- GAPDH (CST, 2118S, 37 kDa,1:10000)

The membrane was incubated with secondary antibodies, and the protein bands were visualized using a chemiluminescence detection system. The original blots/gels are presented in supplementary materials.

The tumor tissues were embedded in paraffin, followed by deparaffinization, antigen retrieval, and blocking. The sections were then incubated with anti-Ki-67 antibody (ZSGB-BIO, ZM-0166), anti-CD4 mAb (CST,25229T) or anti-

CD8αmAb (CST,98951T) overnight at 4°C. Secondary antibody incubation was performed at room temperature, and after dehydration, the slides were mounted with neutral resin and observed under a microscope.

Patients

This study included 30 BLCA patients treated at the Department of Urology, Affiliated Hospital of Guizhou Medical University, between December 2022 and December 2023. Inclusion criteria: (1) Histopathologically confirmed malignant bladder tumor following transurethral resection or radical cystectomy; (2) Availability of paired tumor and adjacent normal tissues (≥2 cm from tumor margin); (3) Complete clinicopathological records (TNM staging, histological grade, pretreatment laboratory values, and postoperative follow-up). Exclusion criteria: (1) Concurrent urological malignancies or metastatic BLCA; (2) Prior neoadjuvant therapy (chemotherapy/radiotherapy/immunotherapy); (3) Severe systemic diseases (uncontrolled diabetes, autoimmune disorders, or active infections). Diagnoses followed the 2024 NCCN Guidelines and Chinese Urological Disease Diagnosis/Treatment Guidelines (2022 edition). TNM staging adhered to AJCC 8th edition standards. The clinical research protocol was approved by the Ethics Committee of the Affiliated Hospital of Guizhou Medical University (Approval Number: 2024141). Written informed consent was obtained from all patients by the Declaration of Helsinki.

Statistical Analysis

Statistical analyses were performed using R software (version 4.2.2) and Perl, with a significance threshold of $P < 0.05$. Paired t-tests were used for paired data comparisons. The chi-square (χ^2) test was used to compare categorical data between two groups. Survival rates between groups were compared using Kaplan-Meier curves and Log rank tests, and Cox proportional hazards regression models were applied for further analysis.

Results

Analysis of IGFL1 Expression Differences in Pan-Cancer

We used the TIMER2.0 database to investigate the expression of IGFL1 across 39 types of cancers, among which 23 had corresponding adjacent normal tissue data available. IGFL1 expression was markedly elevated in tumor tissues in comparison to adjacent normal tissues in BLCA, COAD, CHOL, ESCA, CESC, LUAD, LUSC, READ, THCA, and UCEC. Conversely, the expression of IGFL1 was downregulated in KICH, KIRC, and KIRP (Figure 1A). According to data sourced from TCGA and the GTEx database, IGFL1 expression was significantly elevated in UCEC, BRCA, CESC, LUAD, ESCA, LUSC, BLCA, OV, and PAAD when compared to normal tissues; it was notably downregulated only in TGCT (Figure 1B). The differential expression of IGFL1 across various tumor types suggests it may exert both promotive and inhibitory effects on tumors. Notably, in the TCGA dataset for bladder cancer patients, IGFL1 expression was higher in tumor tissues in contrast to matched adjacent non-tumorous tissues (Figure 1C). Additionally, IGFL1 expression was higher in patients with advanced stages or higher grades of the disease (Figure 1D and E).

Prognostic Value of IGFL1 in Pan-Cancer Survival Analysis

Given the marked dysregulation of IGFL1 across cancers, we next evaluated its clinical relevance through survival analysis. We performed a Cox regression analysis to assess its relationship with OS across various tumor types (Figure 2A). We observed that IGFL1 expression was notably connected to overall survival in multiple cancers, including ACC, CHOL, COAD, HNSC, OV, PCPG, READ, THCA, THYM, UCEC, and UCS. Using the optimal cutoff value of IGFL1 expression, patients were stratified into high and low-expression groups. IGFL1 is a risk factor for poor OS in patients with OV, SARC, HNSC, and PAAD (Figure 2B–E). Additionally, we have assessed the relationship between IGFL1 expression levels and tumor RFS (Figure 2F). IGFL1 was identified as a risk factor for poor RFS in patients with BLCA, KIRC, and HNSC (Figure 2G–I).

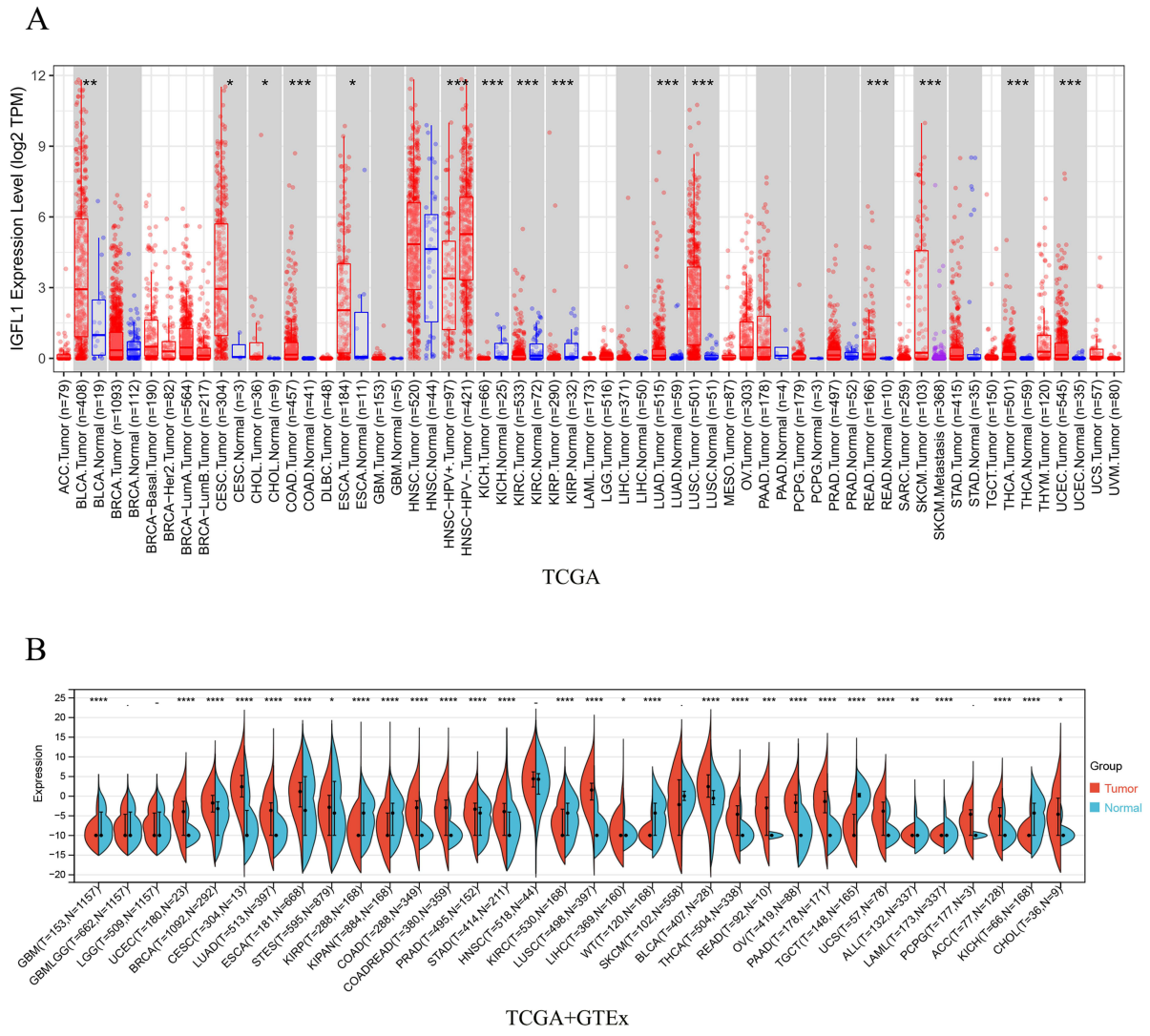

Figure 1 IGFL1 expression in pan-cancer from GEPIA database(**A**). IGFL1 expression in cancer and normal tissues using TCGA and GTEx databases(**B**). Differential expression of IGFL1 in BLCA tissues and paired adjacent non-tumorous tissues(**C**). The correlation of IGFL1 expression and the pathological stages(**D**) and grades(**E**) in BLCA. *P<0.05,**P<0.01,***P<0.001, ****P<0.0001.

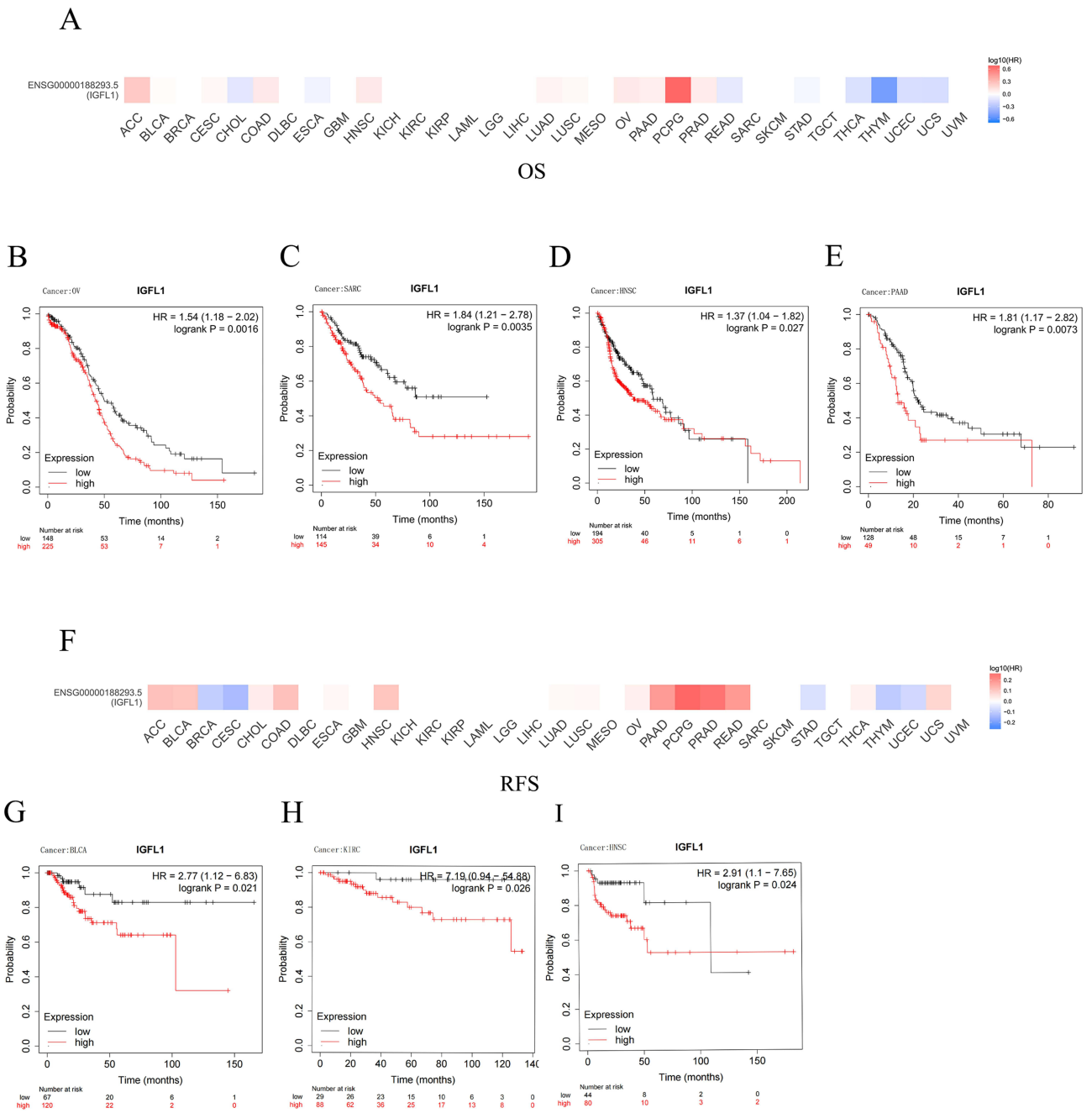

Figure 2 Cox regression analysis of the correlation of IGFL1 with OS(**A**) in various cancers. The prognostic value of IGFL1 on overall survival in OV(**B**), SARC(**C**), HNSC (**D**), PAAD(**E**). Cox regression analysis of the correlation of IGFL1 with RFS(**F**) in various cancers.The prognostic value of IGFL1 on recurrence-free survival in BLCA(**G**), KIRC(**H**), HNSC(**I**).

Association of IGFL1 with Immune Subtypes in Various Cancers

We analyzed the relationship between IGFL1 expression and the six stable and reproducible immune subtypes across various cancers, which include: C1 (wound healing), C2 (IFN-gamma dominant), C3 (inflammatory), C4 (lymphocyte-depleted), C5 (immunologically quiet) and C6 (TGF-beta dominant). The results showed that IGFL1 expression is significantly associated with the immune subtype classification in several cancers, including BLCA, LUSC, LUAD, CESC, SKCM, and BRCA (Figure 3A–F). For instance, in BRCA, IGFL1 expression is highest in the C1 subtype and lowest in the C4 subtype. Additionally, IGFL1 was also correlated with immune subtypes in HNSC, ESCA, UCS, UCEC, READ, OV, PAAD, STAD, CHOL, and COAD (Supplementary Figure 1).

https://doi.org/10.2147/IJGM.S517611

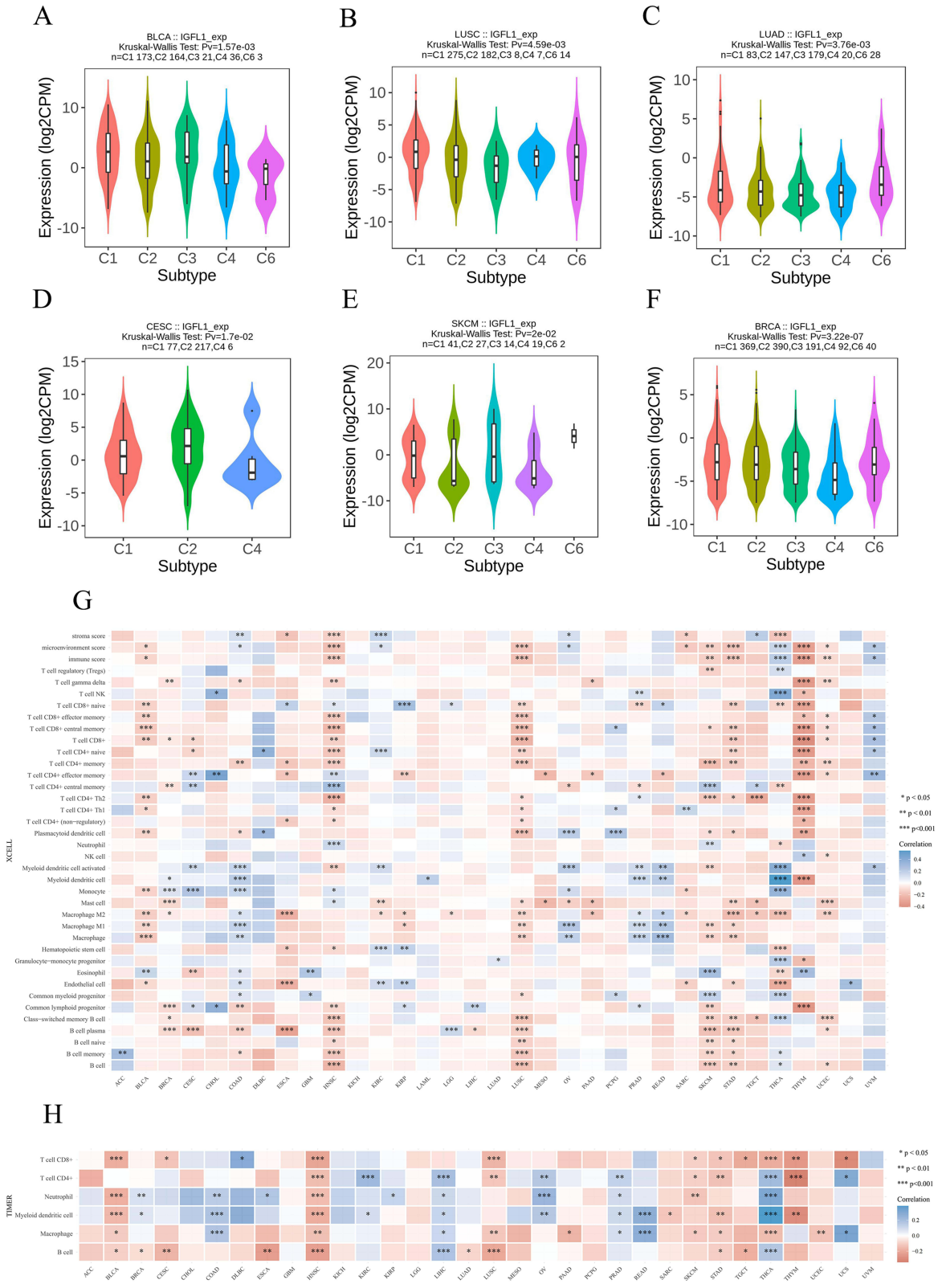

Figure 3 The correlation between the expression of IGFL1 and immune subtypes in BLCA(**A**), LUSC(**B**), LUAD(**C**), CESC(**D**), SKCM(**E**), and BRCA(**F**). Hotmap of IGFL1 expression and the immune cells infiltration in multiple cancers using XCELL(**G**) and TIMER(**H**) database.

Impact of IGFL1 on Tumor Microenvironment (TME)

We assessed the correlation of 38 types of immune cells infiltration using the XCELL database. IGFL1 negatively correlates with numerous immune cells in cancers, including BLCA, BRCA, ESCA, HNSC, LUSC, SKCM, STAD, THYM, and UCEC (Figure 3G). This negative correlation suggests that IGFL1 may play an inhibitory role in the TME, potentially contributing to immune evasion by cancer cells.

We further analyzed the correlation using the TIMER database. IGFL1 was found to be associated with CD8+ T cells in 11 cancer types, CD4+ T cells in 11 types, neutrophils in 11 types, myeloid dendritic cells in 13 types, macrophages in 13 types, and B cells in 11 types of cancer (Figure 3H). Notably, in BLCA, HNSC, LUSC, and STAD, IGFL1 demonstrated an inverse correlation with almost all immune cells, consistent with the findings from the XCELL database. These results indicate that IGFL1 expression significantly influences immune cell infiltration levels.

Additionally, IGFL1 was found to be correlated with immune checkpoint-related genes in several cancers. For instance, in THCA, PRAD, KIRP, and BRCA, IGFL1 revealed a positive relationship with genes involved in immune checkpoints, whereas in TGCT, STAD, SKCM, LGG, and HNSC, it exhibited a more consistent negative correlation (Supplementary Figure 2A). We also evaluated the link between IGFL1 and immunomodulatory genes, including chemokines, chemokine receptors, major histocompatibility complex genes, immune inhibitors, and immunostimulators. IGFL1 showed a positive correlation with several immunomodulatory genes in THCA, KIPAN, BRCA, OV, PAAD, PRAD, LIHC, KIRC, LUAD, and THYM, while it exhibited a negative correlation in TGCT, ESCA, STES, HNSC, LUSC, STAD, and LGG. No significant correlations were observed in UCEC, GBM, LAML, KICH, SKCM, ACC, and MESO (Supplementary Figure 2B).

Relationship Between IGFL1 and Tumor Heterogeneity

Beyond immune modulation, we explored whether IGFL1 contributes to fundamental cancer hallmarks like tumor heterogeneity. Tumor heterogeneity denotes the molecular or genetic changes that occur in tumor cells as they proliferate, leading to variations in growth rate, invasiveness, and drug sensitivity among different tumor cells. We analyzed its association with TMB, MSI, HRD, LOH, MATH, Neoantigen load, and Tumor Purity across various cancers.

IGFL1 was positively associated with TMB in cancers like THYM, KICH, PCPG, ACC, OV, BLCA, PRAD, and PAAD, but negatively in SKCM, SARC, UCS, GBMLGG, LUSC, CHOL, ESCA, and STES (Supplementary Figure 3A). It showed a positive correlation with MSI in KICH, TGCT, ACC, GBMLGG, LIHC, LAML, and SARC but a negative correlation in UCS, SKCM, DLBC, ESCA, and CHOL (Supplementary Figure 3B). IGFL1 was positively correlated with HRD in MESO, KICH, PRAD, OV, LAML, BLCA, STES, COAD, THYM, ACC, LIHC, and COADREAD, but negatively in DLBC, UCS, UVM, LUSC, THCA, LUAD, and READ (Supplementary Figure 3C). It was positively correlated with LOH in PRAD, STES, OV, MESO, PAAD, LIHC, STAD, KIRP, ESCA, CHOL, COAD, TGCT, COADREAD, UVM, and KICH, but negatively in DLBC, THCA, UCEC, UCS, and GBMLGG (Supplementary Figure 3D). IGFL1 correlated positively with MATH in MESO, BLCA, ACC, CESC, DLBC, KICH, LIHC, STES, GBMLGG, LAML, and OV but negatively in ESCA (Supplementary Figure 3E). It was positively correlated with neoantigen load in UVM and READ but negatively in PCPG, KICH, LUAD, and KIRC (Supplementary Figure 3F). IGFL1 showed a positive correlation with tumor purity in THYM, TGCT, ACC, UCS, KICH, and MESO but negative in KIPAN, HNSC, OV, PAAD, COAD, COADREAD, THCA, BRCA, CESC, READ, ESCA, LUAD, SKCM, LUSC, and LIHC (Supplementary Figure 3G). It had a strong positive correlation with tumor stemness scores in THYM, OV, KIRP, THCA, and KIPAN but a negative correlation in TGCT, GBMLGG, and CHOL (Supplementary Figure 3H).

These results highlight the complex effect of IGFL1 in modulating various aspects of tumor heterogeneity, which could have implications for its function in tumorigenesis and cancer progression.

IGFL1 and Anticancer Drug Sensitivity Analysis

Considering IGFL1's multifaceted roles in cancer biology, we performed a Pearson correlation analysis to explore the correlation between IGFL1 expression and the sensitivity to various frequently administered anticancer drugs. The results indicated that IGFL1 expression negatively correlates with the sensitivity to several anticancer agents. This suggests that

higher levels of IGFL1 expression might be associated with resistance to these drugs. We used predictive data from two major drug sensitivity databases for the analysis: the Cancer Therapeutics Response Portal (CTRP) Database (Figure 4A) and the Genomics of Drug Sensitivity in Cancer (GDSC) Database (Figure 4B).

Differential Gene Expression and Enrichment Analysis of Bladder Cancer Cells

Based on pan-cancer associations implicating IGFL1 in bladder cancer (BLCA) progression, we focused mechanistic studies on BLCA models. The RNA sequencing results of the 5637 cell line revealed that, compared to the NC group, knockdown of the IGFL1 gene led to 283 downregulated genes and 516 upregulated genes (Figure 4C). A heatmap illustrated the differences in gene expression and clustering patterns among the samples, with blue representing low expression and red indicating high expression levels. The clustering dendrogram indicated significant variations in gene expression between the NC and Si-IGFL1 groups (Figure 4D). Differentially expressed genes (DEGs) were annotated using EggNOG, showing associations with signaling, transcription, and posttranslational modification, apart from genes with unknown functions (Figure 4E). KEGG pathway annotation analysis identified 84 DEGs associated with the immune system, 73 DEGs categorized under Cancer Overview in the Human Disease pathway, and 110 DEGs involved in signal transduction (Figure 4F).GO annotation and enrichment analysis showed that DEGs were predominantly engaged in binding and catalytic activity, indicating their critical roles in molecular recognition and biochemical reactions. Additionally, they were significantly associated with cellular processes, biological regulation, and metabolic processes, suggesting these genes play key roles in regulating cellular functions and metabolic activities (Figure 4G, 4I). KEGG enrichment analysis highlighted strong associations with Pathways in Cancer, including the JAK/STAT pathway (Figure 4H). Figure 4I illustrates the results of the GO enrichment analysis.

IGFL1 Aberrant Expression in BLCA

To validate bioinformatic predictions, we first confirmed IGFL1 dysregulation in clinical BLCA specimens and cell lines, we retrospectively collected postoperative specimens from 30 bladder cancer patients who underwent surgery at our center. We randomly selected 16 pairs of cancerous tissues and their corresponding adjacent normal tissue counterparts for WB analysis (Figure 5A). The results revealed that IGFL1 was highly expressed in BLCA tissues (Figure 5B). Additionally, when comparing the protein levels of IGFL1 in BLCA cell lines with that in the normal urothelial cell line SVHUC, Western blotting demonstrated significantly higher IGFL1 expression in multiple bladder cancer cell lines (Figure 5C). Consequently, we chose the urothelial carcinoma cell line 5637 and the bladder squamous cell carcinoma cell line ScaBER for subsequent studies. We employed small interfering RNA knockdown and plasmid overexpression of IGFL1 in the 5637 and ScaBER. The efficiency of transfection was validated using qPCR and Western blotting (Figure 5D–F). We selected the siRNA#1 sequence to proceed with subsequent functional experiments.

IGFL1 Promotes EMT in Bladder Tumor Cells

Based on the previous experimental results, we noted a substantial reduction in the proliferative and migratory capacities of bladder tumor cells after IGFL1 knockdown. We examined the linkage between gene expression and EMT to explore the underlying mechanisms, finding a positive correlation in BLCA (Figure 5G). EMT is closely associated with tumor progression, so we further validated the expression of EMT marker proteins in bladder tumor cell lines. Our findings revealed that IGFL1 knockdown elevated E-cadherin expression and decreased in N-cadherin, Vimentin, and Slug expression. Conversely, overexpression of IGFL1 resulted in the opposite changes in these EMT markers (Figure 5H). The results of statistical analysis on the changes in the relative expression levels of EMT marker proteins are shown in Supplementary Fig. 4A-H. These results suggest that IGFL1 regulates EMT in bladder tumor cells, thereby facilitating the malignancy and progression of the disease.

IGFL1 Activates the JAK2/STAT3 Pathway

STAT3 is a critical upstream regulator of the EMT pathway, and multiple studies have confirmed that STAT3 promotes EMT in various cancers.[15,16] IGF1, a homolog of IGFL1, activates STAT3 phosphorylation by specifically binding to its receptor IGF1R.[17] To investigate whether IGFL1 similarly influences STAT3 activation, we conducted a Western blot analysis to assess STAT3 protein changes. Our results showed that the knockdown of IGFL1 led to a decrease in

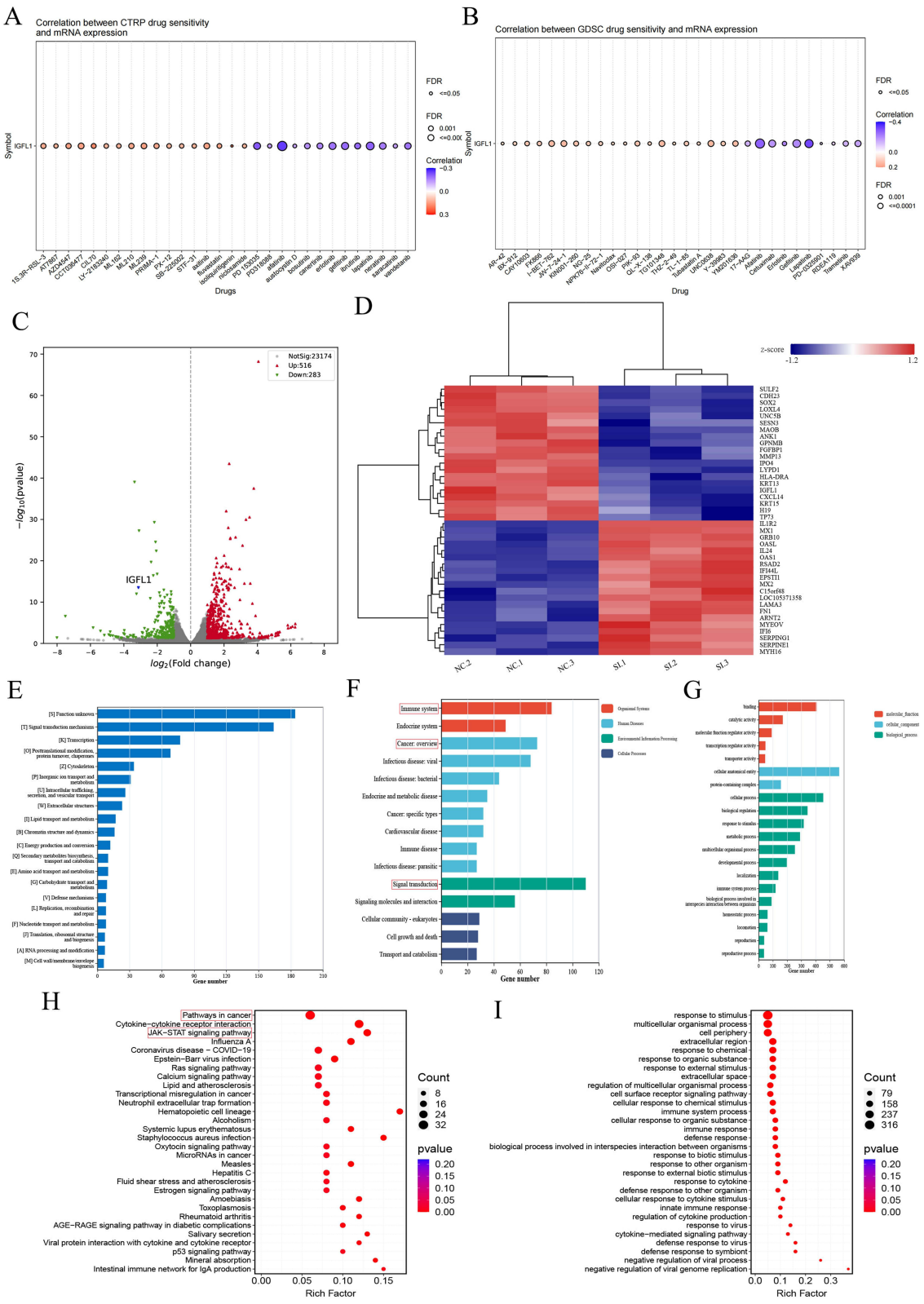

Figure 4 Prediction of anticancer drug sensitivity based on IGFL1 mRNA expression by CTRP(**A**) and GDSC(**B**) database. The volcano plot displays the DEGs after IGFL1 knockdown in 5637 cells (**C**). A heatmap shows the abundance clustering of DEGs (**D**). EggNOG annotation predicts the functions of DEGs (**E**), while KEGG annotation analyzes their functional roles (**F**). GO annotation explores the biological significance of DEGs and their involvement in cellular activities (**G**). KEGG enrichment analysis (**H**) and GO enrichment analysis (**I**) further elucidate the pathways and processes associated with DEGs.

https://doi.org/10.2147/IJGM.S517611

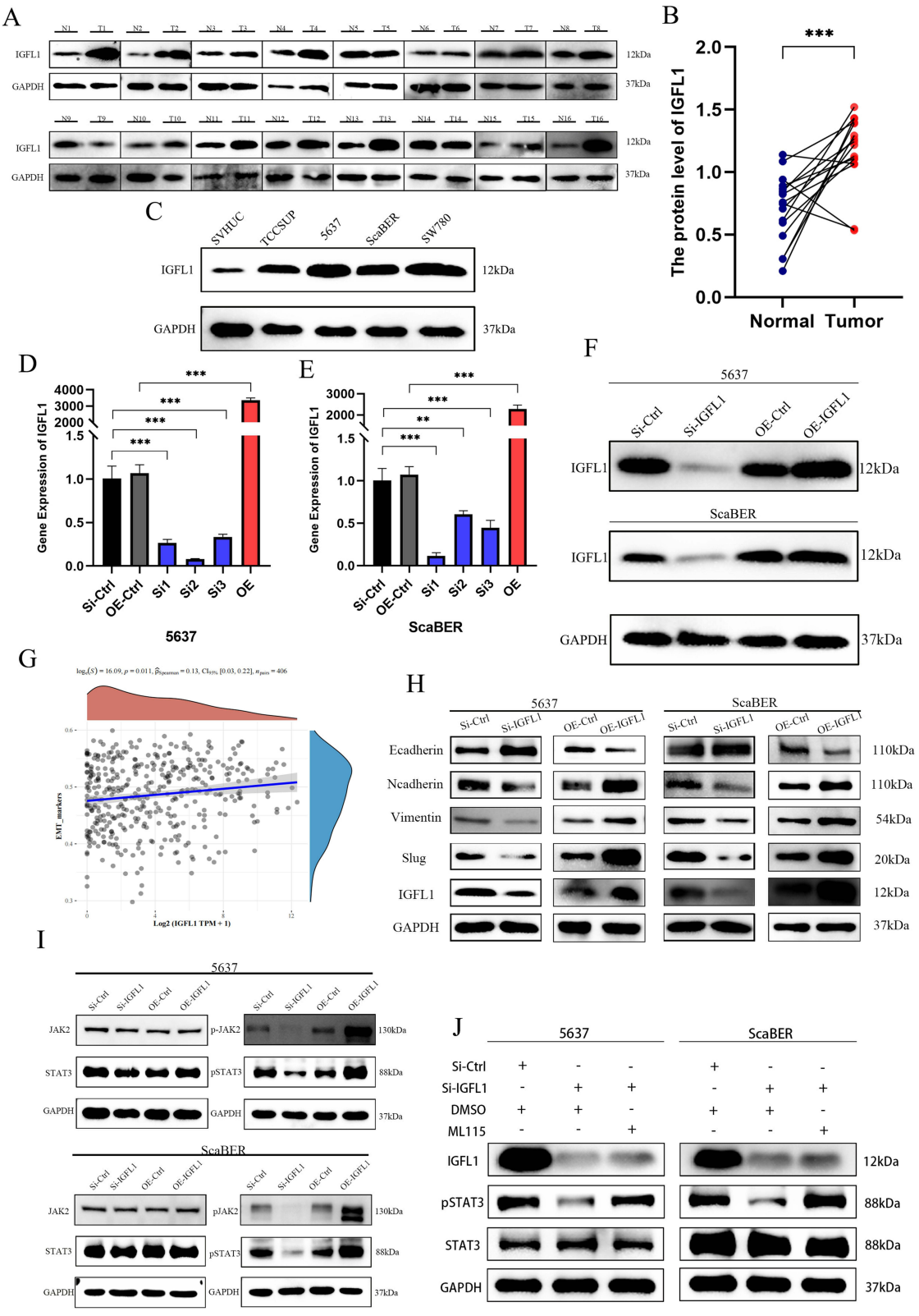

Figure 5 The relative expression of IGFL1 in tissue from BLCA patients (**A**) and statistical analysis of WB(B). The protein expression of IGFL1 in BLCA cell lines contrasts with the normal urothelial cell line (**C**). The mRNA expression of IGFL1 in 5637 (**D**) and ScaBER (**E**) cell lines with knockdown and overexpression. The protein level of IGFL1 in cell lines with IGFL1 knockdown and overexpression (**F**). Spearman's correlation analysis of the correlation of IGFL1 expression and EMT markers (**G**). The protein level of E-cadherin, N-cadherin, Vimentin, and Slug in the IGFL1 knockdown or overexpression in 5637 and ScaBER cell lines (**H**). Western blotting analysis showed that IGFL1 affected the JAK2/STAT3 pathway of BLCA cells (**I**). pSTAT3 level was diminished in IGFL1-knockdown BLCA cell lines 5637 and ScaBER, and this reduction could be rescued by the STAT3 activator ML115 (**J**). Significance was analyzed by two-way ANOVA**P<0.01;***P<0.001.

phosphorylated STAT3 and phosphorylated JAK2 expression, while overexpression of IGFL1 resulted in an increase in phosphorylated STAT3 and phosphorylated JAK2 levels (Figure 5I). We subsequently treated BLCA cell lines infected with IGFL1-knockdown lentivirus with the STAT3 pathway activator ML115 at a concentration of 10 μM. Following treatment, we observed that ML115 rescued the reduction in phosphorylated STAT3 caused by IGFL1 knockdown, while the total STAT3 expression level showed no significant change. (Figure 5J).

IGFL1 Promotes Malignant Biological Behavior of Bladder Tumor Cells in vitro

The CCK8 assay indicated that the proliferation ability of bladder cancer cell lines decreased after IGFL1 knockdown, whereas overexpression of IGFL1 enhanced their proliferative capacity (Figure 6A–D). A wound-healing assay simulated the growth process of tumor cells in surrounding tissues. The shorter the time required for the wound to close, the stronger the migratory ability of the tumor cells. The results showed that bladder tumor cell migration was impaired after IGFL1 knockdown, while overexpression of IGFL1 enhanced migration (Figure 6E–J).We also used a Transwell assay to simulate and assess the migratory ability of tumor cells. The ability of 5637 and ScaBER cells to migrate to the lower chamber was significantly reduced after IGFL1 knockdown (Figure 6K–M).

The STAT3 activator ML115 can rescue the proliferation reduction induced by IGFL1 knockdown in ScaBER cells (Figure 6N) and 5637 cells (Figure 6O). Similarly, ML115 can also rescue the migration impairment caused by IGFL1 knockdown in 5637 cells (Figure 6P) and ScaBER cells (Figure 6Q). These findings imply that IGFL1 is essential in promoting the malignant biological behavior of bladder tumor cells.

IGFL1 Influences Tumor Cell Proliferation in vivo and Regulates the Infiltration of Tumor-Immune Cells

Finally, we extended our findings to in vivo settings to evaluate IGFL1's impact on tumor growth and immune evasion. We generated a BLCA xenograft tumor model (Figure 7A). A significant suppression of tumor growth was observed in the 5637 cell tumors after IGFL1 lentivirus interference (Figure 7B and C).IHC analysis of tumor tissues showed reduced expression of the proliferation marker Ki-67 in the Si-IGFL1 group (Figure 7D). TUNEL staining, which detects fragmented DNA to reflect apoptosis, revealed more apoptotic cells in the Si-IGFL1 group (Figure 7E).

To validate the regulatory effect of IGFL1 on the immune microenvironment, we selected immunocompetent C57 mice and subcutaneously inoculated them with murine bladder cancer cells (MB49) (Figure 7F). The results showed that MB49 tumors overexpressing IGFL1 exhibited significantly faster growth rates than the control group (Figure 7G and H).IHC staining of tumor samples revealed that the experimental group had significantly fewer $CD4^+$ T cells (Figure 7I) and $CD8^+$ T cells (Figure 7J) than the control group, implying that IGFL1 may suppress the infiltration of tumor-immune related cells.

Discussion

The global incidence and mortality rates of cancers have been rising at an alarming pace, posing a severe threat to human health. An estimated 20 million new cancer cases and 9.7 million deaths were recorded in 2022.[1,18] Despite the improvement in various comprehensive cancer treatment strategies, the prognosis for most cancer patients remains unfavorable. Consequently, there is an immediate need to uncover new tumor biomarkers and elucidate their mechanisms in the initiation and progression of tumors to develop more precise diagnostic approaches and therapeutic strategies.

IGFL1 is a member of the human-secreted protein family, situated on chromosome 19q13.32, and encodes a 12 kDa protein. The IGFL family shares high homology with the IGF family, with IGF family members consisting of a signal peptide, A and B chains, and a C peptide. The C peptide connects the A and B chains, varying lengths among family members. The A and B chains are conserved at specific positions, contributing to forming three disulfide bonds: two between the A and B chains (interchain) and one within the A chain (intrachain). The IGFL family retains the intrinsic structure of IGFs but with an inserted segment in the A chain, altering the cysteine motif within the A chain.[4] IGF1 is a well-studied target essential for normal cell metabolism, proliferation, growth, and apoptosis.[19] Numerous studies have also found that IGF1 facilitates tumor growth, including medulloblastoma, prostate cancer, thyroid cancer, and colorectal cancer,[20–23] and mediates tumor drug resistance.[24] Notably, several clinical trials targeting IGF1 for treating human solid

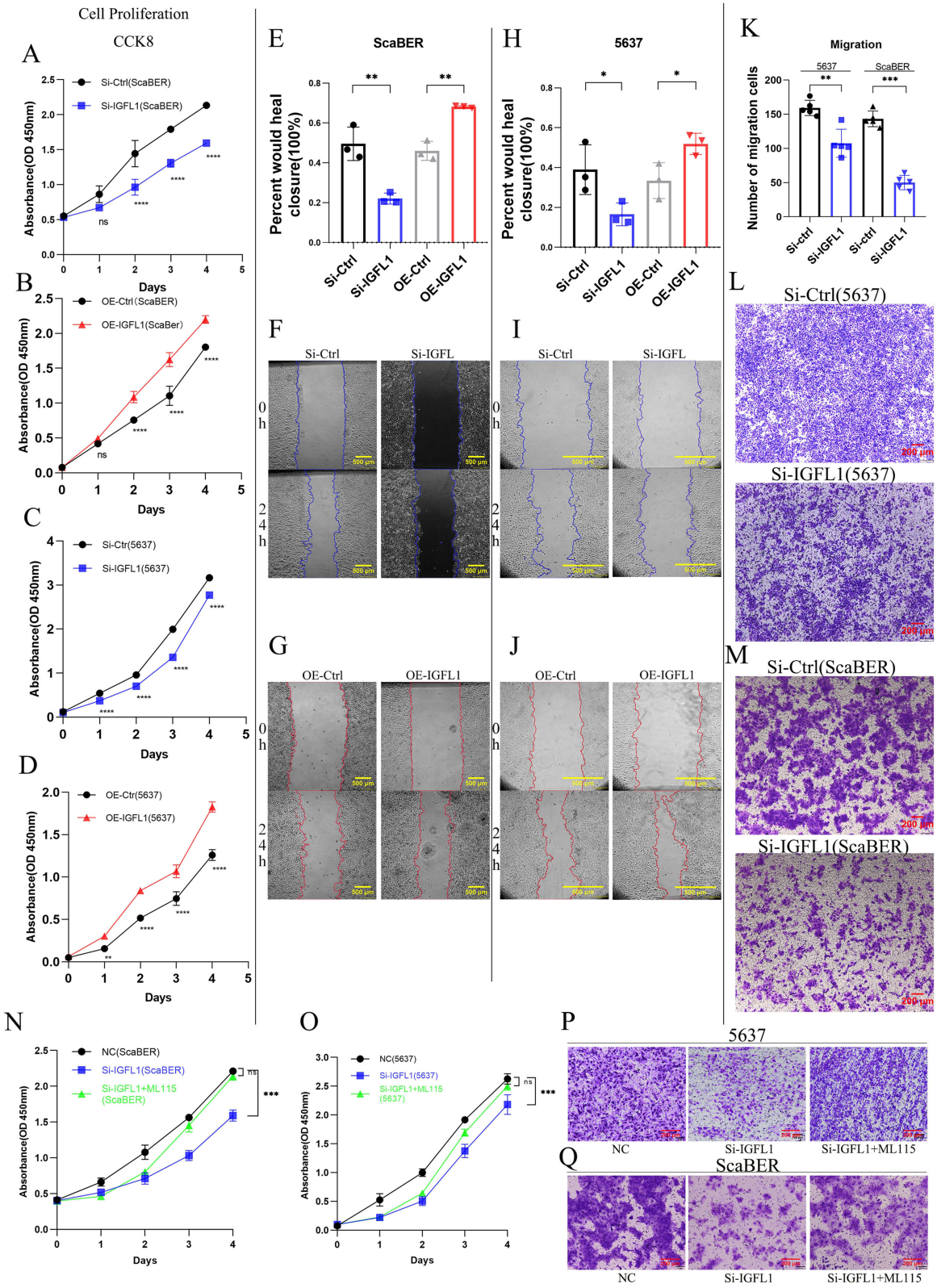

Figure 6 Cell proliferation of 5637 and ScaBER after knockdown and overexpression of IGFL1 (**A–D**). Wound-healing assays showed that IGFL1 affected the migration of ScaBER (**E–G**) and 5637 (**H–J**) cell lines. Transwell assays showed that IGFL1 knockdown inhibited the migration of 5637 (**L**) and ScaBER (**M**), with statistical results (**K**). CC8 rescue experiments were performed in ScaBER (**N**) and 5637 (**O**) cells. Transwell rescue experiments were conducted in 5637 (**P**) and ScaBER (**Q**) cells.Significance was analyzed by two-way ANOVA*P<0.05,**P<0.01,***P<0.001,****P<0.0001.

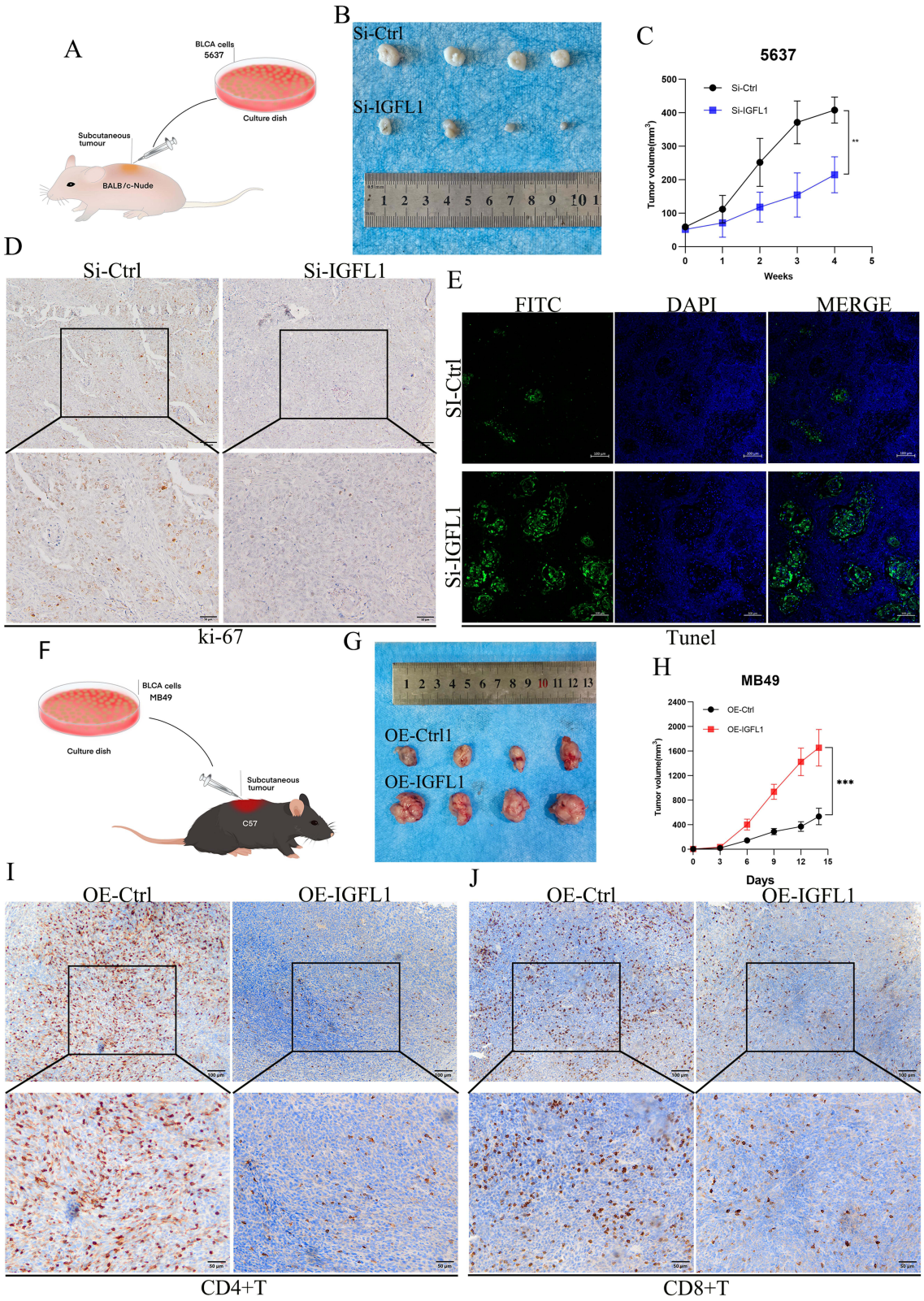

Figure 7 Subcutaneous of 5637 cells in nude mice revealed that xenograft tumor growth was inhibited following infection with IGFL1-interfering lentivirus (**A** and **B**), statistical analysis of tumor volumes (**C**). Ki-67 expression in tumor tissues of the si-IGFL1 group compared to the Si-Ctrl group (**D**). TUNEL staining indicated an increased number of apoptotic cells (**E**). Subcutaneous of MB49 cells in C57 mice showed that xenograft tumor growth was enhanced following infection with IGFL1-overexpression lentivirus (**F** and **G**), statistical analysis of tumor volumes (**H**). Reduction infiltration of CD4+ T cells (**I**) and CD8+ T cells (**J**) in the IGFL1-overexpression group.Significance was analyzed by two-way ANOVA.**P<0.01,***P<0.001.

https://doi.org/10.2147/IJGM.S517611

tumors are currently underway worldwide.[21,25,26] Based on this homology, researchers speculate that IGFL1 may have similar tumorigenic effects and could act as a pan-cancer gene involved in multiple solid tumors. However, no comprehensive research has yet been carried out to explore IGFL1 at the pan-cancer level, and its pro-tumorigenic mechanisms in BLCA remain unclear. In our study, we used bioinformatics techniques to investigate the role of IGFL1 in promoting tumor development, evaluating its relationship with tumor immune subtypes, TMB, MSI, HRD, LOH, MATH, neoantigens, tumor purity, and anticancer drug sensitivity. We also experimentally validated the role and mechanism of IGFL1 in promoting bladder tumor development.

As a potential oncogenic molecule, IGFL1 is abnormally overexpressed in various tumors. In terms of prognosis, high IGFL1 expression is correlated with diminished overall survival in patients with OV, SARC, HNSC, PAAD, and UCEC and shorter progression-free survival in BLCA, KIRC, and HNSC patients. We noted that IGFL1 expression was markedly higher in BLCA tissues compared to adjacent non-cancerous tissues, and patients with higher IGFL1 expression have shorter recurrence-free survival (RFS). As early as 2003, a study involving 154 bladder cancer patients with 154 control patients found that plasma IGF1 levels in BLCA patients were greater than those in controls (175.8 vs 153.2 ng/mL, $p<0.01$).[27] Given that IGFL1 is a homolog of IGF1, it is likely a potential oncogenic molecule in BLCA.

Researchers conducted an immune genomic analysis of 33 cancers, totaling 10,000 tumor samples from the TCGA database, and identified six Immune Subtypes(ISs)(C1-C6). These immune subtypes are closely related to DNA damage, somatic mutations, immune therapy response, and prognosis.[28] Generally, the C3 subtype, characterized by higher expression of inflammation-related genes and abundant immune cell infiltration, is linked to more sensitivity to immune checkpoint inhibitors, while the C2 and C1 subgroups, despite having a high immune component, show poorer outcomes. In contrast, the C4 and C6 subtypes lack antitumor immune responses and have the worst prognosis.[28] We found that IGFL1 is associated with immune subtypes (ISs) across various cancers, with each type exhibiting a unique IS distribution. The tumor and its environment interact continuously, releasing signaling molecules to influence its microenvironment, promoting angiogenesis and immune tolerance.[29] Immune-inflammatory tumors, characterized by high TMB and ample immune cell infiltration, typically respond effectively to immunotherapy. In contrast, immune-exclusion tumors, where immune cells are sparse and mainly located around the tumor, struggle to infiltrate the tumor core. As a result, immune-inflammatory tumors are usually termed “hot tumors”, while immune-exclusion and immune-desert tumors are known as “cold tumors”.[30,31] In certain tumor types, knocking down crucial gene expression has been observed to convert the TME from “cold” to “hot”, thereby enhancing the response to immunotherapy, which could serve as a new anticancer target.[32]

We analyzed whether IGFL1 influences tumor growth and prognosis by affecting the stroma score, microenvironment score, and immune score in the TME. Using the XCELL and TIMER databases, we found that IGFL1 is inversely related to $CD8^+$ T cells in BLCA, CESC, HNSC, LUSC, STAD, THYM, and UCEC, suggesting that IGFL1 expression may suppress $CD8^+$ T cell activity and recruitment, potentially participating in immune evasion mechanisms or inhibiting immune responses. Based on the aforementioned survival analysis results, IGFL1 is more likely to be an oncogenic factor in BLCA and HNSC. Tumor antigens are proteins or peptide molecules specifically expressed by tumor cells, which are internalized and processed by dendritic cells (DCs) and then delivered to T cells. Tumor-specific CD8+ T cells mainly participate in recognizing and eliminating tumors, but in the complex TME, tumor-specific CD8+ T cells often become exhausted.[33,34] To assess the regulatory effect of IGFL1 on immune cell infiltration, we observed notable differences in $CD4^+$ T cell and $CD8^+$ T cell infiltration in xenograft tumors of bladder cancer cells MB49. The expression of IGFL1 was negatively correlated with tumor immune cell infiltration.

Immune checkpoints(IC) are a group of regulatory receptors/ligands tumor cells use to evade immune detection by affecting their expression.[35] Although many drugs targeting ICs have been developed for tumor treatment, only a small proportion of patients respond well, with many developing primary or secondary resistance.[36,37] Tumor immune evasion involves multiple mechanisms, and different ICs play a dominant role in different tumors.[38] Sialic acid-binding Ig-like lectin 15 (SIGLEC15) is a recently discovered IC that is present at reduced levels in most human tissues and various immune subgroups while is highly expressed in highly immunosuppressive tumors, promoting tumor progression by inhibiting CD8+ T cell proliferation.[39,40] Our study found a positive correlation between IGFL1 and SIGLEC15 in UCEC, THCA, READ, PRAP, LUAD, KIRP, KIRC, COAD, BRCA, and BLCA, suggesting a potential mechanism by which IGFL1 may be involved in tumor immune evasion, although more evidence is needed to confirm this.

Furthermore, the correlation between IGFL1 and immune regulatory genes (including chemokines, receptors, MHC, immune inhibitors, and immunostimulators) strengthens the association between IGFL1 and tumor immunity.

Cancer is marked by heterogeneous cells and germline mutations that drive dysregulated cell growth, immune evasion, metabolic dysregulation, and inflammation.[41] Among these, TMB and MSI are well-studied biomarkers that recognize patients who may gain an advantage from immune checkpoint inhibitor (ICI) therapy.[8] High TMB indicates more sites for immune cell recognition, resulting in longer PFS and OS.[8,42] High MSI is an independent risk factor for gastrointestinal tumors' clinical characteristics and prognosis.[43] Our study found that IGFL1 is significantly positively linked to TMB in eight tumors and MSI in seven types, suggesting that high IGFL1 expression in these tumors may lead to better survival outcomes following immunotherapy. Additionally, the CTRP database showed that IGFL1 expression was negatively correlated with the half-maximal inhibitory concentration (IC50) of 13 anticancer drugs, while the GDSC database indicated a negative correlation with ten drugs. Notably, both databases showed a strong negative correlation between IGFL1 and Afatinib and Lapatinib, which are FDA-approved dual inhibitors targeting the epidermal growth factor receptor (EGFR) and human epidermal growth factor receptor 2 (HER2), widely used in cancer treatment.[44,45] HER2 is a member of the tyrosine kinase ERBB family. HER2 amplification/overexpression or somatic mutations are detectable in more than one-fifth of breast cancer patients, and HER2-targeted therapy has benefited this subset of patients.[46] Similar to breast cancer, HER2 amplification/overexpression also occurs in bladder cancer, while HER2 expression is low or undetectable in normal urothelial tissues.[47] Therefore, HER2-targeted therapy holds potential value in the treatment of bladder cancer. In fact, a substantial number of clinical trials have currently evaluated the efficacy and adverse reactions of EGFR/HER2-targeted therapy for urothelial carcinoma.[48,49] Lapatinib can block HER1 and HER2, thereby inhibiting the activation of downstream signaling pathways such as MAPK and PI3K-AKT.[50] In animal models of bladder cancer, it has been found that compared with single use of piroxicam, the combination of lapatinib and piroxicam as first-line treatment exhibits better response rates, survival rates, and adverse reaction profiles.[51] Afatinib, an irreversible pan-HER inhibitor, has been less studied in the treatment of bladder cancer, and major studies have not reached their endpoints.[52] Based on the functions of IGFL1 in tumors and its interactions with drugs, we propose potential strategies for targeting IGFL1 as a therapeutic target, including the development of monoclonal antibodies, small-molecule inhibitors, or gene therapy approaches against IGFL1. These strategies are expected to enhance the sensitivity of tumor cells to existing drugs by regulating IGFL1 expression or function, thereby improving therapeutic efficacy.

BLCA represents a form of malignant neoplasm with the highest frequency of gene mutations, and its molecular characteristics are strongly linked with the prognosis of BC.[53,54] Being the leading malignancy of the urinary tract, particularly in advanced stages, treatment options for BLCA are limited.[55] Therefore, we focused on BLCA and validated the elevated expression of IGFL1 in bladder tumor tissues using postoperative specimens. Knockdown or overexpression of the IGFL1 gene resulted in altered proliferation and migration abilities of bladder cancer cells, accompanied by changes in EMT-related marker proteins. In vivo experiments yielded the same results. Through RNA sequencing results, we found that IGFL1 is associated with various tumor pathways, with significant enrichment observed in the JAK/STAT3 pathway. STAT3, a central node in numerous oncogenic signaling pathways, is activated in bladder tumors, where it forms a dimer with phosphorylated STAT3 (pho-STAT3) via its SH2 domain, subsequently translocating to the nucleus to interact with DNA response elements, thereby regulating the cell cycle, proliferation, and apoptosis.[56,57] Besides, STAT3 plays a crucial role in inducing immunosuppression within the TME.STAT3 recruits immunosuppressive Tregs, B cells, and M2 macrophages while inhibiting dendritic cells' maturation, activation, and antigen presentation.[58] Research by Zong et al has shown that IGF1 can activate STAT3 phosphorylation in various cell lines and tissues at different developmental stages in mice.[17] We subsequently examined changes in JAK2/STAT3 pathway activity following alterations in IGFL1 levels. After IGFL1 knockdown, p-JAK2/p-STAT3 expression decreased, whereas overexpression of IGFL1 led to increased p-JAK2/p-STAT3 levels. Applying the STAT3 activator ML115 can rescue the STAT3 inhibition and the weakened proliferation and migration abilities caused by IGFL1 knockdown. Considering these findings, we hypothesize that IGFL1 may promote EMT in bladder cancer cells through the STAT3 pathway. However, its role in regulating immune infiltration and immune evasion remains under investigation, and further experimental studies are required to validate IGFL1 as a therapeutic target.

Despite our comprehensive characterization of IGFL1's role in pan-cancer, our study has certain limitations. Some of the analyses are solely based on bioinformatics and predictions related to tumor immunity have not been experimentally validated. Additionally, we have only confirmed IGFL1's oncogenic role in BLCA. In vitro and in vivo experiments were performed using a limited set of cell lines (5637, ScaBER, MB49) and a retrospective cohort of 30 clinical specimens. This sample size, though sufficient for initial validation, may introduce selection bias and limit generalizability to broader BLCA subtypes. Future studies should expand validation to larger, multi-center clinical cohorts encompassing diverse molecular subtypes of BLCA and other cancer types. Given the breakthroughs achieved with its homolog IGF1 in cancer therapy, we believe that IGFL1 is also a promising target for tumor immunotherapy, warranting further in-depth research.

Conclusion

Our study comprehensively analyzed the correlation between IGFL1 expression and various factors in cancer patients, including prognosis, immune subtypes, immune cell infiltration, immune checkpoint genes, TMB, MSI, HRD, LOH, MATH, neoantigens, tumor purity, and anticancer drug sensitivity. Furthermore, experimental validation demonstrated that IGFL1 promotes proliferation, migration, and EMT in bladder cancer cells. This is the first study to investigate IGFL1 across multiple cancers, and our findings propose that IGFL1 could be a promising therapeutic target.

Data Sharing Statement

The authors will make the raw data supporting the findings of this study available upon reasonable request. All raw data supporting the conclusions of this article will be freely accessed in public database.

Ethics Statement

The clinical research protocol was approved by the Ethics Committee of the Affiliated Hospital of Guizhou Medical University (Approval Number: 2024141). Written informed consent was obtained from all patients by the Declaration of Helsinki. The animal experiment was approved by the Animal Experimental Ethical Inspection Form of Guizhou Medical University (Approval Number: 2305143). All procedures involving mouse subcutaneous tumorigenesis were conducted in accordance with the Guide for the Care and Use of Laboratory Animals (US National Academy of Sciences).

Acknowledgments

We appreciate the TCGA database and R software for free use.

Author Contributions

All authors made a significant contribution to the work reported, whether that is in the conception, study design, execution, acquisition of data, analysis and interpretation, or in all these areas; took part in drafting, revising or critically reviewing the article; gave final approval of the version to be published; have agreed on the journal to which the article has been submitted; and agree to be accountable for all aspects of the work.

Funding

This study was funded by the National Natural Science Foundation of China (Number: 82060462, 82360558), The Science and Technology Foundation of Guizhou Province (Number: ZK[2023] 211, ZK[2023]-205, gzwjrs2024-006), The Foundation of Health and Family Planning Commission of Guizhou Province (Number: gzwkj2021-057, gzwjkj2014-1-002, gzwkj2023-038),and The Foundation of Guizhou Provincial Administration of Traditional Chinese Medicine (QZYY-2024-007). The funding agencies and donors had no role in any aspect of this study.

Disclosure

The authors declare no commercial or financial relationships that could be perceived as a potential conflict of interest in the conduct of this research. All authors have consented to the publication of this manuscript.

References

1. Bray F, Laversanne M, Sung H. et al. Global cancer statistics 2022: GLOBOCAN estimates of incidence and mortality worldwide for 36 cancers in 185 countries. *CA Cancer J Clin*. 2024;74(3):229–263. doi:10.3322/caac.21834
2. Bejarano L, Jordão MJC, Joyce JA. Therapeutic targeting of the tumor microenvironment. *Cancer Discovery*. 2021;11(4):933–959. doi:10.1158/2159-8290.Cd-20-1808
3. Bagaev A, Kotlov N, Nomie K, et al. Conserved pan-cancer microenvironment subtypes predict response to immunotherapy. *Cancer Cell*. 2021;39(6):845–865.e7. doi:10.1016/j.ccell.2021.04.014
4. Emtage P, Vatta P, Arterburn M, et al. IGFL: a secreted family with conserved cysteine residues and similarities to the IGF superfamily. *Genomics*. 2006;88(4):513–520. doi:10.1016/j.ygeno.2006.05.012
5. Rajput M, Kujur PK, Mishra A, Singh RP. Flavonoids inhibit chronically exposed arsenic-induced proliferation and malignant transformation of HaCaT cells. *Photodermatol Photoimmunol Photomed*. 2018;34(1):91–101. doi:10.1111/phpp.12357
6. Wang Z, Liang X, Wang X, Yu Q. Elevated expression of IGFL1 indicates unfavorable prognosis in lung adenocarcinoma through promotion of cell proliferation and inhibition of apoptosis. *Polish J Pathol*. 2021;72(4):283–295. doi:10.5114/pjp.2021.114174
7. Wang H, Shi Y, Chen CH, et al. KLF5-induced lncRNA IGFL2-AS1 promotes basal-like breast cancer cell growth and survival by upregulating the expression of IGFL1. *Cancer Lett*. 2021;515:49–62. doi:10.1016/j.canlet.2021.04.016
8. Galvano A, Gristina V, Malapelle U, et al. The prognostic impact of tumor mutational burden (TMB) in the first-line management of advanced non-oncogene addicted non-small-cell lung cancer (NSCLC): a systematic review and meta-analysis of randomized controlled trials. *ESMO open*. 2021;6(3):100124. doi:10.1016/j.esmoop.2021.100124
9. Wilbur HC, Le DT, Agarwal P. Immunotherapy of MSI cancer: facts and hopes. *Clin Cancer Res*. 2024;30(8):1438–1447. doi:10.1158/1078-0432.Ccr-21-1935
10. Doig KD, Fellowes AP, Fox SB. Homologous recombination repair deficiency: an overview for pathologists. *Modern Pathol*. 2023;36(3):100049. doi:10.1016/j.modpat.2022.100049
11. Westphalen CB, Fine AD, André F, et al. Pan-cancer analysis of homologous recombination repair-associated gene alterations and genome-wide loss-of-heterozygosity score. *Clin Cancer Res*. 2022;28(7):1412–1421. doi:10.1158/1078-0432.Ccr-21-2096
12. Wu X, Song P, Guo L, Ying J, Li W. Mutant-allele tumor heterogeneity, a favorable biomarker to assess intra-tumor heterogeneity, in advanced lung adenocarcinoma. *Front Oncol*. 2022;12:888951. doi:10.3389/fonc.2022.888951
13. Xie N, Shen G, Gao W, Huang Z, Huang C, Fu L. Neoantigens: promising targets for cancer therapy. *Signal Transduc Targeted Therapy*. 2023;8(1):9. doi:10.1038/s41392-022-01270-x
14. Deng Y, Song Z, Huang L, et al. Tumor purity as a prognosis and immunotherapy relevant feature in cervical cancer. *Aging*. 2021;13(22):24768–24785. doi:10.18632/aging.203714
15. Sadrkhanloo M, Entezari M, Orouei S, et al. STAT3-EMT axis in tumors: modulation of cancer metastasis, stemness and therapy response. *Pharmacol Res*. 2022;182:106311. doi:10.1016/j.phrs.2022.106311
16. Jin W. Role of JAK/STAT3 signaling in the regulation of metastasis, the transition of cancer stem cells, and chemoresistance of cancer by epithelial-mesenchymal transition. *Cells*. 2020;9(1):217. doi:10.3390/cells9010217
17. Zong CS, Chan J, Levy DE, Horvath C, Sadowski HB, Wang LH. Mechanism of STAT3 activation by insulin-like growth factor I receptor. *J Biol Chem*. 2000;275(20):15099–15105. doi:10.1074/jbc.M000089200
18. Han B, Zheng R, Zeng H, et al. Cancer incidence and mortality in China, 2022. *J National Cancer Center*. 2024;4(1):47–53. doi:10.1016/j.jncc.2024.01.006
19. Wang M, Pugh SM, Daboul J, Miller D, Xu Y, Hill JW. IGF-1 acts through kiss1-expressing cells to influence metabolism and reproduction. *bioRxiv*. 2024. doi:10.1101/2024.07.02.601722
20. Yao M, Ventura PB, Jiang Y, et al. Astrocytic trans-differentiation completes a multicellular paracrine feedback loop required for medulloblastoma tumor growth. *Cell*. 2020;180(3):502–520.e19. doi:10.1016/j.cell.2019.12.024
21. Cagigas ML, Fiorito G, Bertozzi B, et al. Effects of protein restriction on insulin-like growth factor (IGF)-1 in men with prostate cancer: results from a randomized clinical trial. *Biomarker Res*. 2024;12(1):68. doi:10.1186/s40364-024-00613-w
22. Chen LH, Xie T, Lei Q, Gu YR, Sun CZ. A review of complex hormone regulation in thyroid cancer: novel insights beyond the hypothalamus-pituitary-thyroid axis. *Front Endocrinol*. 2024;15:1419913. doi:10.3389/fendo.2024.1419913
23. Kasprzak A. Insulin-like growth factor 1 (IGF-1) signaling in glucose metabolism in colorectal cancer. *Int J Mol Sci*. 2021;22(12):6434. doi:10.3390/ijms22126434
24. Basu R, Kopchick JJ. GH and IGF1 in cancer therapy resistance. *Endocrine-Related Cancer*. 2023;30(9). doi:10.1530/erc-22-0414
25. Soria JC, Massard C, Lazar V, et al. A dose finding, safety and pharmacokinetic study of AVE1642, an anti-insulin-like growth factor-1 receptor (IGF-1R/CD221) monoclonal antibody, administered as a single agent and in combination with docetaxel in patients with advanced solid tumours. *Eur J Cancer*. 2013;49(8):1799–1807. doi:10.1016/j.ejca.2013.01.003
26. Carcaboso AM. Results from the children's oncology group Phase III trial of a monoclonal antibody against the insulin-like growth factor-1 receptor in patients with newly diagnosed metastatic Ewing sarcoma. *Transl Pedia*. 2023;12(10):1916–1919. doi:10.21037/tp-23-388
27. Zhao H, Grossman HB, Spitz MR, Lerner SP, Zhang K, Wu X. Plasma levels of insulin-like growth factor-1 and binding protein-3, and their association with bladder cancer risk. *J Urol*. 2003;169(2):714–717. doi:10.1097/01.ju.0000036380.10325.2a
28. Thorsson V, Gibbs DL, Brown SD, et al. The immune landscape of cancer. *Immunity*. 2018;48(4):812–830.e14. doi:10.1016/j.immuni.2018.03.023
29. Pagadala M, Sears TJ, Wu VH, et al. Germline modifiers of the tumor immune microenvironment implicate drivers of cancer risk and immunotherapy response. *Nat Commun*. 2023;14(1):2744. doi:10.1038/s41467-023-38271-5
30. Zhang J, Huang D, Saw PE, Song E. Turning cold tumors hot: from molecular mechanisms to clinical applications. *Trends Immunol*. 2022;43(7):523–545. doi:10.1016/j.it.2022.04.010
31. Galon J, Bruni D. Approaches to treat immune hot, altered and cold tumours with combination immunotherapies. *Nat Rev Drug Discovery*. 2019;18(3):197–218. doi:10.1038/s41573-018-0007-y
32. Wu J, Hu W, Yang W, et al. Knockdown of SQLE promotes CD8+ T cell infiltration in the tumor microenvironment. *Cell Signalling*. 2024;114:110983. doi:10.1016/j.cellsig.2023.110983

33. Dolina JS, Van Braeckel-Budimir N, Thomas GD, Salek-Ardakani S. CD8(+) T cell exhaustion in cancer. *Front Immunol*. 2021;12:715234. doi:10.3389/fimmu.2021.715234
34. Wang Q, Qin Y, Li B. CD8+ T cell exhaustion and cancer immunotherapy. *Cancer Lett*. 2023;559:216043. doi:10.1016/j.canlet.2022.216043
35. Khan M, Arooj S, Wang H. NK cell-based immune checkpoint inhibition. *Front Immunol*. 2020;11:167. doi:10.3389/fimmu.2020.00167
36. Chen DS, Mellman I. Oncology meets immunology: the cancer-immunity cycle. *Immunity*. 2013;39(1):1–10. doi:10.1016/j.immuni.2013.07.012
37. Charoentong P, Finotello F, Angelova M, et al. Pan-cancer immunogenomic analyses reveal genotype-immunophenotype relationships and predictors of response to checkpoint blockade. *Cell Rep*. 2017;18(1):248–262. doi:10.1016/j.celrep.2016.12.019
38. Lei X, Lei Y, Li JK, et al. Immune cells within the tumor microenvironment: biological functions and roles in cancer immunotherapy. *Cancer Lett*. 2020;470:126–133. doi:10.1016/j.canlet.2019.11.009
39. Wang J, Sun J, Liu LN, et al. Siglec-15 as an immune suppressor and potential target for normalization cancer immunotherapy. *Nature Med*. 2019;25(4):656–666. doi:10.1038/s41591-019-0374-x
40. Kang FB, Chen W, Wang L, Zhang YZ. The diverse functions of Siglec-15 in bone remodeling and antitumor responses. *Pharmacol Res*. 2020;155:104728. doi:10.1016/j.phrs.2020.104728
41. Chang MT, Asthana S, Gao SP, et al. Identifying recurrent mutations in cancer reveals widespread lineage diversity and mutational specificity. *Nature Biotechnol*. 2016;34(2):155–163. doi:10.1038/nbt.3391
42. Palmeri M, Mehnert J, Silk AW, et al. Real-world application of tumor mutational burden-high (TMB-high) and microsatellite instability (MSI) confirms their utility as immunotherapy biomarkers. *ESMO open*. 2022;7(1):100336. doi:10.1016/j.esmoop.2021.100336
43. Gryfe R, Kim H, Hsieh ET, et al. Tumor microsatellite instability and clinical outcome in young patients with colorectal cancer. *New Engl J Med*. 2000;342(2):69–77. doi:10.1056/nejm200001133420201
44. Yang JC, Schuler M, Popat S, et al. Afatinib for the treatment of NSCLC harboring uncommon EGFR mutations: a database of 693 cases. *J Thoracic Oncol*. 2020;15(5):803–815. doi:10.1016/j.jtho.2019.12.126
45. Yuan Y, Liu X, Cai Y, Li W. Lapatinib and lapatinib plus trastuzumab therapy versus trastuzumab therapy for HER2 positive breast cancer patients: an updated systematic review and meta-analysis. *Syst Rev*. 2022;11(1):264. doi:10.1186/s13643-022-02134-9
46. Oh DY, Bang YJ. HER2-targeted therapies - a role beyond breast cancer. *Nat Rev Clin Oncol*. 2020;17(1):33–48. doi:10.1038/s41571-019-0268-3
47. Drago JZ, Modi S, Chandarlapaty S. Unlocking the potential of antibody-drug conjugates for cancer therapy. *Nat Rev Clin Oncol*. 2021;18(6):327–344. doi:10.1038/s41571-021-00470-8
48. Xu J, Zhang H, Zhang L, et al. Real-world effectiveness and safety of RC48-ADC alone or in combination with PD-1 inhibitors for patients with locally advanced or metastatic urothelial carcinoma: a multicenter, retrospective clinical study. *Cancer Med*. 2023;12(23):21159–21171. doi:10.1002/cam4.6680
49. Patelli G, Zeppellini A, Spina F, et al. The evolving panorama of HER2-targeted treatments in metastatic urothelial cancer: a systematic review and future perspectives. *Cancer Treat Rev*. 2022;104:102351. doi:10.1016/j.ctrv.2022.102351
50. Nagano M, Kohsaka S, Ueno T, et al. High-throughput functional evaluation of variants of unknown significance in ERBB2. *Clin Cancer Res*. 2018;24(20):5112–5122. doi:10.1158/1078-0432.Ccr-18-0991
51. Maeda S, Sakai K, Kaji K, et al. Lapatinib as first-line treatment for muscle-invasive urothelial carcinoma in dogs. *Sci Rep*. 2022;12(1):4. doi:10.1038/s41598-021-04229-0
52. Choudhury NJ, Campanile A, Antic T, et al. Afatinib activity in platinum-refractory metastatic urothelial carcinoma in patients with ERBB alterations. *J Clin Oncol*. 2016;34(18):2165–2171. doi:10.1200/jco.2015.66.3047
53. Alexandrov LB, Nik-Zainal S, Wedge DC, et al. Signatures of mutational processes in human cancer. *Nature*. 2013;500(7463):415–421. doi:10.1038/nature12477
54. Nadal R, Bellmunt J. Management of metastatic bladder cancer. *Cancer treatment reviews*. *Jun*. 2019;76:10–21. doi:10.1016/j.ctrv.2019.04.002
55. Compérat E, Amin MB, Cathomas R, et al. Current best practice for bladder cancer: a narrative review of diagnostics and treatments. *Lancet*. 2022;400(10364):1712–1721. doi:10.1016/s0140-6736(22)01188-6
56. Mirzaei S, Gholami MH, Mahabady MK, et al. Pre-clinical investigation of STAT3 pathway in bladder cancer: paving the way for clinical translation. *Biomed Pharmacothe*. 2021;133:111077. doi:10.1016/j.biopha.2020.111077
57. Alcantara MB, Tang WS, Wang D, et al. Targeting STAT3 in tumor-associated antigen-presenting cells as a strategy for kidney and bladder cancer immunotherapy. *Front Immunol*. 2023;14:1274781. doi:10.3389/fimmu.2023.1274781
58. Zou S, Tong Q, Liu B, Huang W, Tian Y, Fu X. Targeting STAT3 in cancer immunotherapy. *Mol Cancer*. 2020;19(1):145. doi:10.1186/s12943-020-01258-7